Pergamon

Geochimica et Cosmochimica Acta, Vol. 68, No. 3, pp. 443–454, 2004

0016-7037/04 $30.00 + .00

doi:10.1016/S0016-7037(03)00455-1

Surface chemistry and relative Ni sorptive capacities of synthetic hydrous Mn oxyhydroxides under variable wetting and drying regimes

CORRIE KENNEDY,[1] D. SCOTT SMITH,[2] and LESLEY A. WARREN[1,*]

[1]School of Geography and Geology, McMaster University, Hamilton, ON, Canada
[2]Department of Chemistry, Wilfrid Laurier University, Waterloo, ON, Canada

(*Received September* 10, 2002; *accepted in revised form June* 19, 2003)

Abstract—The surface binding site characteristics and Ni sorptive capacities of synthesized hydrous Mn oxyhydroxides experimentally conditioned to represent three hydrological conditions—MnO_{XW}, freshly precipitated; MnO_{XD}, dried at 37°C for 8 d; and MnO_{XC}, cyclically hydrated and dehydrated (at 37°C) over a 24-h cycle for 7 d—were examined through particle size analysis, surface acid-base titrations and subsequent modelling of the pK_a spectrum, and batch Ni sorption experiments at two pH values (2 and 5). Mineralogical bulk analyses by XRD indicate that all three treatments resulted in amorphous Mn oxyhydroxides; i.e., no substantial bulk crystalline phases were produced through drying. However, drying and repeated wetting and drying resulted in a non-reversible decrease in particle size. In contrast, total proton binding capacities determined by acid-base titrations were reversibly altered with drying and cyclically re-wetting and drying from 82 ± 5 μmol/m^2 for the MnO_{XW} to 21 ± 1 μmol/m^2 for the MnO_{XD} and 37 ± 5 μmol/m^2 for the MnO_{XC}. Total proton binding sites measured decreased by ≈75% with drying from the MnO_{XW} and then increased to ≈50% of the MnO_{XW} value in the MnO_{XC}. Thus, despite a trend of higher surface area for the MnO_{XD}, a lower total number of sites was observed, suggesting a coordinational change in the hydroxyl sites. Surface site characterization identified that changes also occurred in the types and densities of surface sites for each hydrologically conditioned Mn oxyhydroxide treatment (pH titration range of 2–10). Drying decreased the total number of sites as well as shifted the remaining sites to more acidic pK_a values. Experimentally determined apparent pH_{zpc} values decreased with drying, from 6.82 ± 0.06 for the MnO_{XW} to 3.2 ± 0.3 for the MnO_{XD} and increased again with rewetting to 5.05 ± 0.05 for the MnO_{XC}. Higher Ni sorption was observed at pH 5 for all three Mn oxyhydroxide treatments compared to pH 2. However, changes in relative sorptive capacities among the three treatments were observed for pH 2 that are not explainable simply as a function of total binding site density or apparent pH_{zpc} values. These results are the first to our knowledge, to quantitatively link the changes induced by hydrologic variability for surface acid base characteristics and metal sorption patterns. Further, these results likely extend to other amorphous minerals, such as Fe oxyhydroxides, which are commonly important geochemical solids for metal scavenging in natural environments.

1. INTRODUCTION

Defining the important geochemical solids for reactive metal transport in aquatic systems has been of increasing interest for environmental geochemistry (e.g., Tessier et al., 1996; Fein et al., 1997; Warren and Ferris, 1998; Cox et al., 1999; Nelson et al., 1999a; Matocha et al., 2001). With the growing recognition that, in addition to oxyhydroxide minerals of iron, organic matter and bacteria are key players controlling metal reactions, modelling efforts have moved beyond simple representations of pure mineral surfaces to more complex approaches which aim to reflect the heterogeneous reality of natural sorbents. The importance of organic solids, whether live or dead, has been emphasized in low pH systems, where these types of sorbents would be more effective as metal sorbents than Fe oxyhydroxides, due to the presence of carboxylic groups on organic surfaces which render them negatively charged even at the lowest pH values. In contrast, the hydroxyl surface groups of Fe oxyhydroxides typically show pK_a values in the circumneutral range making them less effective in low pH systems (Dzombak and Morel, 1990; Robertson and Leckie, 1998).

Results from investigation into natural systems, have highlighted the need for more quantitative investigations into other potentially relevant geochemical sorbents. Mn oxyhydroxides, often amorphous, are commonly found to be important metal sorbents in field studies (Catts and Langmuir, 1986; Tessier et al., 1996; Tebo et al., 1997; Robertson and Leckie, 1998; Lee et al., 2002). However, in laboratory investigations, crystalline forms of Mn oxyhydroxides, such as birnessite, have been used as reference Mn oxide model compounds in surface complexation modelling (Appelo and Postma, 1999) and metal sorption experiments (Loganathan and Burau, 1973). Given the environmental importance of amorphous Fe oxyhydroxides in determining metal behaviour (e.g., hydrous ferric oxide, HFO, or ferrihydrite; Kukier and Chaney, 2000; Parmar et al., 2001; Trivedi and Axe, 2001) and the typical amorphous nature of Mn oxyhydroxides in soils (Fritsch et al., 1997), amorphous Mn oxyhydroxides are likely to have significant environmental relevance where they occur. There is a growing body of literature that examines the formation of Mn oxyhydroxides, principally by microbial catalysis in aquatic systems (e.g., Emerson et al., 1982; Mandernack et al., 1995; Nelson et al., 1999b; Emerson, 2000), but their role as reactive surfaces has only recently been quantitatively examined (Trivedi and Axe, 2001; Trivedi et al., 2001). In contrast to oxyhydroxides of iron,

* Author to whom correspondence should be addressed (warrenl@mcmaster.ca).

those of Mn are thought to possess a negative surface charge at much lower pH values (pH_{zpc} 2.3; Catts and Langmuir, 1986), and thus, like organic surfaces may play a more significant role in metal sorption than Fe oxyhydroxides in low pH systems.

Acid mine drainage (AMD) is a significant environmental issue for both metal and acidity contamination. A seemingly paradoxical characteristic of AMD environments, given their harsh reality (pH values commonly well below 4, metal loads in the micromolar to molar ranges; Lee et al., 2002; Haack and Warren, 2003), is the existence of thriving microbial populations (Bond et al., 2000; Kusel and Dorsch, 2000; Leveille et al., 2001). In a field investigation of the biogeochemical linkages controlling metal dynamics in AMD tailings associated seepage streams, our research group has observed that Mn oxyhydroxides play a key role in metal sequestration (Haack and Warren, 2003). Under low pH conditions, the existence of amorphous Mn oxyhydroxides is predominantly controlled by microbial genesis, as their abiotic precipitation rates are extremely slow at pH values < 8, unlike Fe oxyhydroxides, which will oxidize and precipitate readily at pH values as low as 3 (Schwertmann and Cornell, 1991).

An important question that has not been addressed in the literature, is the potential changes that might occur in Mn oxyhydroxide crystallinity and/or surface characteristics given the extremely variable water levels experienced by such shallow seepage streams and the typically small, amorphous nature of the particles themselves. Such effects are likely to be of more widespread importance to natural systems than just AMD environments and Mn oxyhydroxides in particular. The amorphous nature and small size commonly observed in natural particles makes them susceptible to changes in a variety of environmental conditions such as water content, redox state, and temperature. The potential influence of such impacts on solid characteristics as well as associated impacts for metal reactivity must be characterized if accurate representations of metal behaviour in natural systems are to be developed.

The focus, therefore, of this laboratory study was to quantitatively examine the influence of variable hydrologic conditions on mineralogy, particle morphology, surface characteristics and sorptive capacity of synthetic Mn oxyhydroxides. Three experimental systems designed to represent three differing hydrologic regimes were evaluated: (1) wet, freshly precipitated, amorphous Mn oxyhydroxides (MnO_{XW}); (2) dried Mn oxyhydroxides (MnO_{XD}): and (3) cycled Mn oxyhydroxides that were cyclically exposed to wet and dry conditions (MnO_{XC}). Particle size characteristics were determined by laser particle size analyses. Surface site types and densities were determined by acid-base titration and modeled using the FOCUS method (Smith and Ferris, 2003). Nickel sorptive capacities of the three Mn oxyhydroxide treatments were evaluated by batch sorption experiments.

2. MATERIAL AND METHODS

2.1. Preparation of Mn Oxyhydroxide

In all outlined experimental procedures, all reagents used were of reagent grade and all glass/plasticware was acid washed with 3 to 5% HCl and rinsed with ultra pure water (UPW, 18 MΣ) five times before use. Amorphous Mn oxyhydroxides were precipitated in the laboratory following the methods established by Nelson et al. (1999a) and Murray (1974). The resulting synthesized Mn oxyhydroxide precipitate was pelleted by centrifugation (10 min at 10,000 rpm, Sorvall RC5C+ ultracentrifuge), and then washed three times with UPW. The precipitate was then divided into three experimental systems: (1) MnO_{XW}, wet, freshly precipitated Mn oxyhydroxide; (2) MnO_{XD}, Mn oxyhydroxide dried at 37°C for 8 d; and (3) MnO_{XC}, Mn oxyhydroxide dried at 37°C for 24 h, then hydrated for 24 h, with the wetting/drying cycle repeated three times, over 7 d.

2.2. Mineralogy and Crystallinity

Three samples were collected from each Mn oxyhydroxide experimental system for mineralogical analyses by X-ray powder diffraction analyses (XRD, Siemens Diffractometer D5005 using Cu-Kα radiation) after hydrologic conditioning. These samples were air dried in an anaerobic chamber (95% N_2:5% H_2 atmosphere) for 48 h before analyses. Scans were run for 5 h to ensure that most, if not all phases were analyzed and samples were run using a zero background holder to reduce background noise. In addition, backscattered electron imaging was used to identify phases/minerals. Particles from the three treatments were visually inspected by environmental scanning electron microscopy (ESEM; ESEM system 2020, Version 3.53, FEI Co.). Mean particle surface areas were determined from laser particle size analyses (LPSA, Coulter LS230C Lazer Fluid Module, Beckman Coulter, FL). All particle surface area estimation techniques are operational: LPSA was chosen since analyses can be performed on wet samples in contrast to the commonly used, N_2 gas adsorption technique, BET, which requires drying of the sample. Whilst LPSA may underestimate SA in comparison to the more widely used BET technique (i.e., geometric surface area vs. reactive surface area); we chose it due to the lower likelihood of method artifacts in the surface area estimates derived. As results discussed subsequently show, our LPSA derived results agree well with other published estimates derived from BET analyses.

2.3. Titration Procedure

Mn oxyhydroxides from each of the three hydrologic scenarios were first washed with the electrolyte to be used in subsequent acid-base titrations (0.1-mol/L KNO_3) and then centrifuged as above, before titration. All samples were titrated under an N_2 atmosphere using an automatic Mettler Toledo DL70 interfaced by DLWin software to a personal computer. The titrations were run on dynamic mode that adds variable amounts of titrant to maintain approximately equal pH intervals. All reagents (0.1-mol/L HCl and 0.1-mol/L NaOH) and electrolyte (0.1-mol/L KNO_3) were prepared in an anaerobic chamber (95% N_2:5% H_2 environment) to prevent contact of any reagent with CO_2.

The titration cups containing the samples were also prepared in an anaerobic chamber immediately before titrating. Titrations were run under 0.1-mol/L ionic strength (KNO_3) and the pH was adjusted to ~9 by adding small, known increments of 0.1-mol/L NaOH (standardized using potassium hydrogen phthalate). The cup was then removed from the chamber and attached to the closed system of the titrator. N_2 was bubbled into the cup for 5 min before initializing the titration procedure. Ascarite towers were used to prevent any atmospheric CO_2 from coming into contact with the aqueous sample. The method was then initialized and the sample was titrated using 0.1-mol/L HCl down to a pH of ~2.5. A blank titration using UPW was conducted on the KNO_3 to calibrate the electrode into concentration units.

To analyze these data, chemical equilibrium is assumed but was not specifically tested for. To test for chemical equilibrium, forward (up in pH) and reverse (down in pH) titrations would have to overlap exactly with no hysteresis. For the current work, it was decided to make chemical equilibrium an assumption applied to all titrations, but it should be noted that this is an operationally defined chemical equilibrium and not necessarily "true equilibrium." The comparisons among treatments are still valid as all titrations were run under identical conditions.

2.4. Modelling Approach: FOCUS

The experimental data were fit to a smooth continuous pK_a spectrum using the Fully Optimized Continuous (FOCUS) pK_a technique. Details

are given in Smith and Ferris (2003) but a brief description is given below. To fit the data, equilibrium is assumed and the surface is represented as a sum of monoprotic sites with monoprotic dissociation reactions. First the data are transformed to the charge excess expression. Then the charge excess data are fit to a model for the proton-interface system. The charge excess from the data for the *i*th addition of titrant is shown in Eqn. 1 below:

$$b_{i,meas} = \frac{Cb_i - Ca_i + [H^+]_i - [OH^-]_i}{C_s} \quad (1)$$

where $b_{i,\mathrm{meas}}$ is the charge excess (in μmol/mg of solid), Cb_i, and Ca_i are the concentrations of base and acid added respectively and the final two terms in the numerator are the proton and hydroxyl concentrations in solution, determined using the glass electrode. Finally, C_s is the solid concentration (in mg/L).

There are many options for how to fit this transformed data (Brassard et al., 1990; Nederlof et al., 1994; Cerník et al., 1995), but for our purposes here it was decided that a continuous model for the proton binding was desirable to facilitate comparisons between samples. In addition, a continuous model is more representative of the natural heterogeneity expected on the mineral surfaces. The mathematical model for the data at the *i*th titration point, as transformed in Eqn. 1, is presented in Eqn. 2:

$$b_{i,calc} = \sum_{j=1}^{m} \frac{K_j L_{Tj}}{K_j + [H^+]} + S^o \quad (2)$$

The modelling here ignores electrostatic effects and thus the determined parameter values are ionic strength dependent. A pK_a spectrum represents the overall proton binding of the surface as a summation of monoprotic dissociation reactions, each reaction being defined by a unique pK_a value (K_j in Eqn. 2) and a corresponding site concentration (L_{Tj} in Eqn. 2). In addition, to account for the possibility of positive charge on the surface there is a constant offset term S_o. To determine a pK_a spectrum, first the pK_a values are defined on a sequence from some minimum to some maximum value at fixed step sizes. Thus, the pK_a values are fixed and what remains is to assign concentrations to each of *m* sites such that the data is described as follows for *n* titration points:

$$\mathrm{Ax} = \mathrm{b}$$

$$\text{where } \mathrm{A}(i,j) = \frac{K_j}{K_j + [H^+]_i} \text{ for i} = 1 \ldots \text{n and j} = 1 \ldots \text{m}$$

$$\text{and A } (i,j) = 1 \text{ for i} = 1 \ldots \text{n and j} = \text{m} + 1 \quad (3)$$

There is an $n \times (m + 1)$ matrix **A** of α terms, an $(m + 1) \times 1$ vector of site concentrations, **x** where the final entry is a constant offset term S_o (see Eqn. 2). The stability constants K_j are defined from the disassociation reaction of each monoprotic site with corresponding $pK_{aj} = -\log_{10}K_{aj}$. The $n \times 1$ vector of measured charge excess terms is defined as **b**. A traditional least-squares approach to this problem would vary the parameters in **x** to minimize the sum of the squares of the difference between the calculated and measured value for **b**. However, mathematically the problem is ill-posed (Press et al., 1992). This is because many solutions can describe the data equivalently well and a slight change in the data results in a large change in the fitted parameters. Cerník et al. (1995) have applied a regularization method of solving ill-posed problems to acid-base titration data. Regularization involves using some a priori information about the system to further constrain the results; this leads to less sensitivity to data changes. One constraint imposed by the nature of the system is that all of the ligand concentrations must be positive. In addition, the results can be regularized for a few discrete sites or for smoothness depending on if a discrete or continuous result is desired. Here we use regularization for smoothness. This a priori assumption about the nature of the final result makes it possible to formulate the regularized least-squares optimization problem for *n* titration points:

$$\text{minimize SS} + \lambda R$$

$$\text{where } SS = \sum_{i=1}^{n} (b_{calc,i}(x) - b_{meas,i})^2$$

$$\text{and R}(x_1, \ldots, x_m) = \sum_{j=2}^{m-1} (x_{j-1} - 2x_j + x_{j+1})^2 \text{ and x} \geq 0. \quad (4)$$

The *SS* term is the usual sum of squares term for nonlinear regression; without regularization only this term would be minimized. The regularization term is also dependent on the values of the parameter vector and the regularization power is controlled by the constant λ. The *R* function corresponds to the sum of squares of finite difference approximation of the second derivatives. This function is small for smoothly varying values of **x** and large if the values of **x** oscillate.

There are two values to optimize for the minimization problem defined in Eqn. 4, both the smoothness and the goodness of fit. Theoretically, there is an optimal answer that satisfies both criteria with a minimum of compromise in the other (Press et al., 1992). Determining this optimal solution depends on the regularization strength given by the parameter λ. Smith and Ferris (2003) present a method to optimize the parameter λ such that both the goodness of fit and regularization are best satisfied. This method involves defining two axes, one for *SS* and one for λR values. In this space the origin is defined as the optimal answer to the sum of squares problem and the regularization problem independent of the other problem. The optimal answer is determined by varying λ, and calculating new values of *SS* and λR, to minimize the distance from this new point to the origin, and in this way, optimally satisfying both criteria. Because both goodness-of-fit and smoothness are optimized, this is termed the Fully Optimized Continuous (FOCUS) pK_a spectrum method. All data were analyzed using Matlab (The MathWorks Inc., Natick, MA). Parameter fitting was performed using the Optimization Toolbox within Matlab.

2.5. Nickel Sorption Experiments

Batch Ni sorption experiments were run for each of the three hydrologically conditioned Mn oxyhydroxides. Mn oxyhydroxides for the Ni sorption experiments were prepared in an identical manner to those used in the acid base titrations. Three replicate batch systems for each of the three Mn oxyhydroxide treatments were exposed to a nominal concentration of 0.01-mol/L Ni using ~80 mg of Mn oxyhydroxide (equivalent dry weight) for two different pH values (2 and 5) for 24 h. Blank UPW and standard (Ni solution 0.01 mol/L; no sorbent) systems were also run to account for any contamination or loss of Ni to the container walls. The closed bottles were placed on an orbital shaker (Forma Scientific, 150 rpm), and gently shaken under atmospheric conditions for 24 h. Over the first 8 h, the pH was monitored and adjusted every 30 to 60 min. The pH was also adjusted again after a total of 20 h. After 24 h, at the end of the experiment, the final pH was recorded without adjustment and the bottles were centrifuged (Sorvall RC-5C+ ultracentrifuge, 30 min at 10,000 rpm). After centrifugation, the supernatant was recovered from each bottle using acid-washed syringes and syringe filtered (0.45 and 0.2 μm; Nucleopore Acrodisc 25-mm syringe filter, Pall Gelman Laboratory, Ann Arbor, MI) directly into sample containers and subsequently acidified to 0.2% HNO_3 v/v (Fisher Scientific OPTIMA HNO_3, Seastar Chemicals Inc., Sidney, Canada) before analyses for nickel and dissolved Mn content by inductively coupled plasma mass spectrometry (ICP-MS). The amount of Ni sorbed in each batch system was determined from both direct solid analyses as well as from supernatant differences in Ni concentration at the start and end of the experiment to account for any Ni loss to the container walls. Supernatant Ni concentrations were determined as the difference between the Ni content of the original stock solution (corrected for both [1] sorptive losses experienced by the Ni standard systems and [2] any Mn oxyhydroxide mass loss due to mineral dissolution; both were negligible, i.e., $< 5\%$ for [1] and $< 2.0\%$ for [2]) and the final solution Ni concentration for each bottle. Solid associated Ni concentrations were determined directly by digestion of the pelleted MnOx solid in each of the bottles using a microwave digestion system (Ethos Plus, Milestone Inc., Bergamo, Italy) and the protocol outlined

Table 1. Physical characteristics of the three hydrological MnOx treatments.

	Particle size distribution expressed as a percentage of the total particles			Surface area ($m^2\ g^{-1}$)	Crystallinity
	$<0.2\ \mu m$	0.2–2.0 μm	$>2.0\ \mu m$		
MnO_{XW}	0.35 ± 0.04	0.65 ± 0.04	0.0035 ± 0.003	41 ± 1	Amorphous
MnO_{XD}	0.48 ± 0.02	0.52 ± 0.02	0.00091 ± 0.00002	45 ± 2	Amorphous
MnO_{XC}	0.45 ± 0.02	0.55 ± 0.02	0.00133 ± 0.00009	47 ± 3	Amorphous

Errors shown are S.E.

by Haack and Warren (2003) for amorphous oxyhydroxides, with 0.25-mol/L hydroxylamine hydrochloride in 25% (v/v) acetic acid and analyses for Ni and Mn by ICP-MS. Even though observed Ni and Mn losses were small, reported Ni concentrations associated with Mn oxyhydroxides are corrected for any calculated loss of either element as treatment dependent effects were observed. All metal data are reported as mean values plus or minus one standard error (S.E.) defined as the standard deviation divided by the square root of sample size or *n* (Zar, 1984).

In this study, statistical significance is defined as values that fall outside the range of plus or minus one standard error of each other.

3. RESULTS AND DISCUSSION

3.1. Mn Oxyhydroxide Mineralogy and Morphology

No detectable crystalline structural changes were induced either by drying of Mn oxyhydroxides at 37°C, or repeatedly wetting and drying of these materials over a 7-d period; all three Mn oxyhydroxides treatments were determined to be amorphous using X-Ray Diffractrometry (XRD; Siemens D5005 Xray diffractometer using zero background holder for a 5-h scan to attempt to detect any crystalline phases present; scans not shown). Our lack of XRD detectable crystallite formation in association with aging is consistent with Luo et al. (2000), who also showed no formation of crystalline phases for synthetic Mn oxyhydroxides under very similar conditions to our study (40°C for 12 d). The temperature selected in our study for drying of the Mn oxyhydroxides preparations (37°C) was chosen to reflect the maximum temperatures recorded in the field AMD site; and thus our protocol is representative of processes that occur in natural systems over a seasonal timescale. These results suggest that detectable bulk changes in crystallinity would only occur over longer timescales in natural low temperature surface environments. Visual inspection of the three Mn oxyhydroxide treatments by environmental scanning electron microscopy (ESEM; results not shown) revealed fine-grained, amorphous particles for all three treatments, consistent with the XRD results indicating no significant crystallinity. It should be noted that any surficial structural changes that may have occurred are not resolvable via standard XRD analyses.

The mean surface areas ($m^2\ g^{-1}$) and associated standard errors calculated from particle size analyses indicated a trend of increasing surface area with increased hydrological conditioning from wet (41 ± 1 $m^2\ g^{-1}$) to dry (45 ± 2 $m^2\ g^{-1}$) to cycle (47 ± 3 $m^2\ g^{-1}$; Table 1). These estimated values agree well with those published in the literature for abiotically precipitated synthetic Mn oxyhydroxides, determined by BET analysis, ranging between 32 and 56 $m^2\ g^{-1}$ (Nelson et al., 1999a; Matocha et al., 2001; Nelson et al., 2002). This comparison indicates that LPSA and BET derived estimates of surface area do not necessarily widely differ from each other.

The observed differences in surface area among the three Mn oxyhydroxide treatments, are consistent with observed changes in particle size induced by drying and cyclically rewetting and drying, which shifts the particle size spectra to smaller particles (Table 1). All the treatments resulted in extremely fine-grained particles, with > 99% of the total particle size spectrum $< 2\mu m$ in size. However, drying of the Mn oxyhydroxides significantly increased the proportion of particles $< 0.2\ \mu m$ in size from 35% in the wet treatment to 48% in the dry. The MnO_{XC} particle size spectrum was not significantly different from the MnO_{XD}, but both were significantly different from the MnO_{XW}, indicating that particle size changes are not reversible with re-wetting. From these results, it might be expected that more hydrologically conditioned Mn oxyhydroxides would exhibit higher sorption capacities for a given mass, due to a proportional increase in surface area and associated density of surface functional groups.

3.2. Surface Characteristics

Plots of the titration data transformed as the charge excess expression (Eqn. 1) show that the three MnOx treatments differ significantly in the nature of their proton binding (Fig. 1). Furthermore, each MnOx treatment set of replicate results show good reproducibility indicating robust surface characteristics. A comparison of the actual data (indicated by the symbols, Fig. 1 and the model fits to the data (indicated by the lines) show extremely good agreement. Thus the model results used to determine site densities and pK_a values can reasonably be assumed to accurately reflect the entire range in surface protonation over the titratable range for these three Mn oxyhydroxide treatments.

The physical characteristics of the three MnOx treatments indicated amorphous particles that differed somewhat in particle size and therefore relative surface area associated with a given mass for each treatment. Thus, based on the physical characteristics, it might be expected that the total number of surface sites would increase with hydrological conditioning from wet through dry to cycle preparations as surface area increased with this conditioning. Given the changes in surface area associated with the hydrological conditioning, modelling results were calculated both on an areal, as well as on a mass basis (to permit comparison to other literature estimates). On both an areal and mass basis, the results for the total number of binding sites contradict the expected results from the physical characteristics. Modelling results indicate both the total number

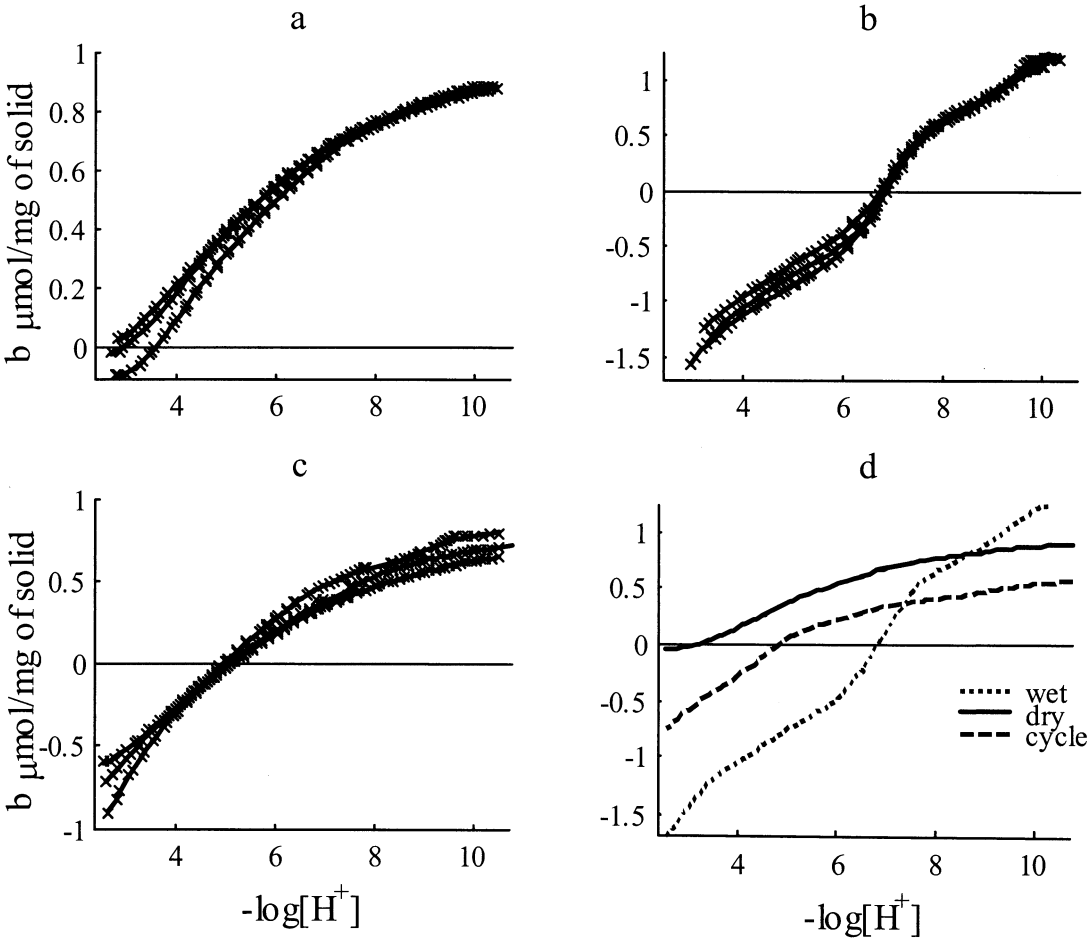

Fig. 1. Titration data transformed as the charge excess per mg of solid. Subplots a, b and c are for dry, wet and cycle data respectively. The x symbols represent measured data points and the solid lines represent the best-fit results for each data set. In subplot (d) the lines represent the average models for the indicated solids obtained by taking the average pK_a spectrum results for each replicate titration data set.

of surface sites, as well as the number of types and associated densities, differ amongst treatments (Fig. 2; Tables 2 and 3). However, the total proton binding capacity in the measured pH range (2–10) decreases with hydrological conditioning. The results show that drying of the Mn oxyhydroxides actually lowers the number of surface sites in this range whilst increasing relative surface area (Tables 1 and 2), However, in contrast to particle size and associated surface area characteristics, which do not appear to show reversibility with cycled hydrologic conditioning (Table 1), the total proton binding capacity appears sensitive to hydrologic conditioning as is evident by the intermediate total binding capacity value of the MnO_{XC} treatment. This result indicates that the total number of sites increases with repeated wetting and drying (Tables 1 and 2) whilst the surface area does not. Thus, particle size and associated surface area are affected by the drying phase of conditioning, and are not reversible given re-wetting, whilst surface site characteristics appear to be dynamically affected by rewetting.

The total site density decreases with drying, by ≈75% from 82 ± 5 μmol/m^2 for the MnO_{XW} to 21 ± 1 μmol/m^2 for the MnO_{XD}, but subsequently increased with rewetting by ≈50% to 37 ± 5 μmol/m^2 for the MnO_{XC}. When site densities are calculated as a function of mass, the results show the same pattern of decreasing with drying from MnO_{XW} to MnO_{XD} (3.4 ± 0.2 to 0.96 ± 0.04 μmol/mg), and increasing again with rewetting to 1.8 ± 0.2 for the MnO_{XC} (Table 2). These results indicate that both mass and surface area normalizations in this study give the same interpretation of surface acid base characteristics with hydrologic conditioning.

Results also indicate that a number of different surface hydroxyl groups occur; ranging between five to six discrete types across the treatments (Table 3). Differing types of surface hydroxyl groups have commonly been noted for amorphous and crystalline Fe oxyhydroxides (Cerník et al., 1996, Venema et al., 1998; Smith and Ferris, submitted). These studies, which have typically identified between four and six discrete hydroxyl groups, are consistent with our results for Mn oxyhydroxides. These results indicate that surface hydroxyl group variability is likely a common occurrence for oxide mineral surfaces. It is not possible with these amorphous solids to indicate specifically which surface sites are reacting, but the types of sites have been

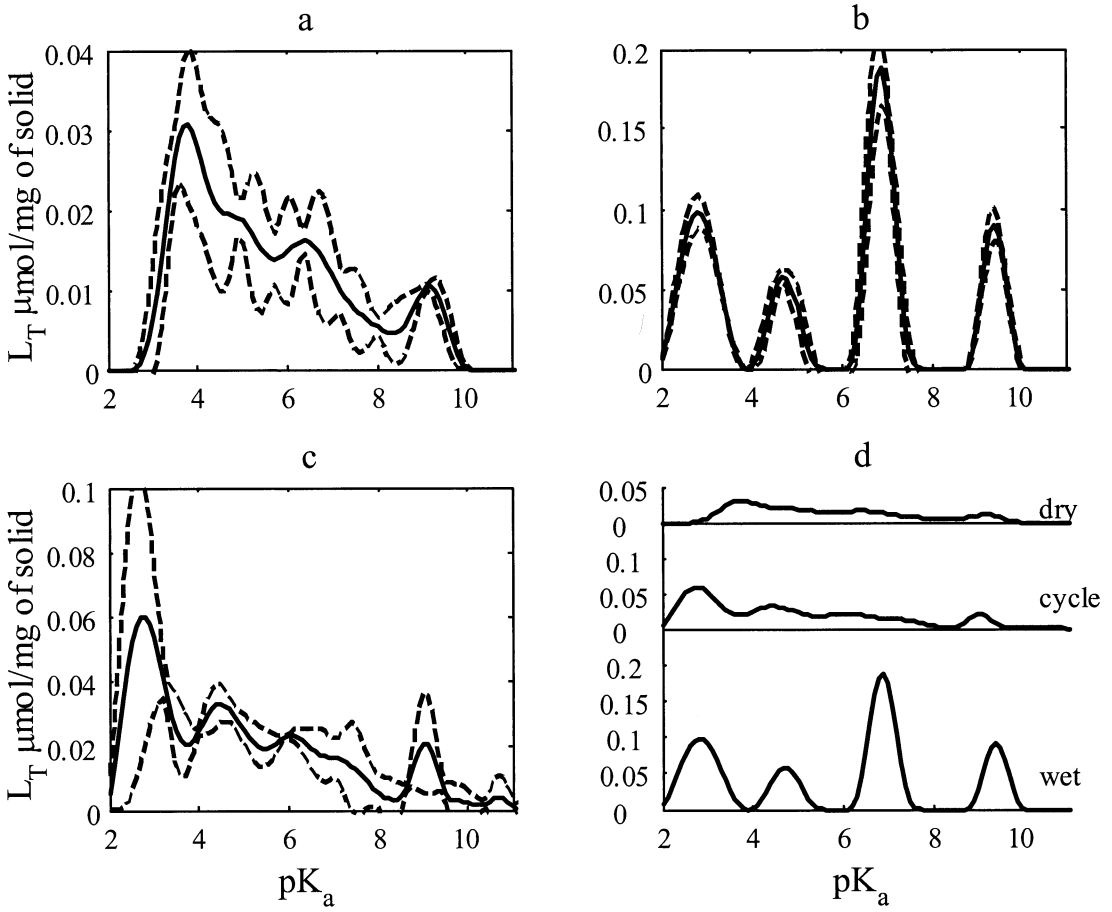

Fig. 2. pK_a spectrum for each treatment. Subplots (a), (b) and (c) correspond to dry, wet and cycle data respectively. The solid line for each treatment represents the mean value of the three replicate titrations and the dotted lines represent one standard deviation about the mean. Subplot (d) shows the mean pK_a spectra for each indicated treatment.

summarized into type I, II, III and IV for pK_a ranges 2 to 4, 4 to 6, 6 to 8 and 8 to 10. Plots of the concentrations of deprotonated sites for these ranges of pK_a values clearly show differences for the three types of hydrologically conditioned Mn oxyhydroxides (Fig. 3).

The distribution of sites is also substantially affected by hydrological conditioning (Table 3). The MnO_{XW} had the lowest number of types of sites with very discrete pK_a values, associated with four distinct peaks over the titrated range (very high reproducibility between replicate titrations). In contrast, the MnO_{XC} and MnO_{XD} show a greater number of less distinct peaks (higher variability between replicate titrations; Fig. 2, Table 3). Three types of sites are consistent across all three treatments however, with pK_a values of ~4 to 4.5, 6.6 to 6.9 and 9 to 9.1 (Table 3). The results observed for the MnO_{XD} and MnO_{XC} indicate dynamic shifting of the pK_a ranges observed, e.g., a strong acid site observed for the MnO_{XW} with a pK_a of ~2.8 is lost in the MnO_{XD}, but re-appears in the MnO_{XC} (Table 3). Thus, these results show that some surface sites are extremely stable whilst others appear, disappear and re-appear with drying and re-wetting associated with the hydrological conditioning. The reduction of sites as a result of drying is not proportional across the titrated range; rather, results indicate a higher loss from the more basic types (Table 3). Similar to the MnO_{XW}, the MnO_{XC} has the two most acidic types of sites as well as the most basic type of site; however the densities for these site types are much lower for the MnO_{XC}. In addition, the MnO_{XC} shows similar variability to the MnO_{XD}, with less discrete pK_a values and fewer sites than the MnO_{XW}.

The wet and dry preparations show the greatest difference, while the cycle preparation bears some resemblance to both, indicating hydrologic effects on surface site type and densities are apparently reversible. That is, surface topography is sensitive to hydrologic conditioning, reducing the total number of sites associated with the surface, and dynamically affecting the types of surface sites that occur.

Table 2. Total binding capacity within the titratable range of pH 2 to 10.

	Total binding capacity	
	µmol/mg	µmol/m^2
MnO_{XW}	3.4 ± 0.2	82 ± 5
MnO_{XD}	0.96 ± 0.04	21 ± 1
MnO_{XC}	1.8 ± 0.2	37 ± 5

Table 3. Sites identified for each of the three hydrological treatments.

	$2 < pK_a \leq 4$ type I	$4 < pK_a \leq 6$ type II	$6 < pK_a \leq 8$ type III	$pK_a > 8$ type IV	Number of sites	S_o (μmol/mg)
MnO_{XW}	2.82	4.72	6.88	9.04	4	–2.1 ± 0.1
MnO_{XD}	3.60	4.06, 5.00	6.59, 7.95	9.12	6	–0.07 ± 0.03
MnO_{XC}	2.77	4.50, 5.99	6.90	9.05, 10.60	6	–1.0 ± 0.2

In addition to pK_a values and binding site concentrations, Table 3 also includes values for the offset term, S_o. This term corresponds to how much the titration curve has to be shifted so that the changes in shape can be represented as a sum of monoprotic negatively charged sites; i.e., to the acid neutralizing capacity (Brassard et al., 1990). Alternatively, it can be thought of as the difference between the proton binding sites that are always saturated and those that are always empty over the titration range. Because this term is a difference between two unknown quantities it cannot be used in any quantitative way to compare titration curves. However, the apparent zero-point of charge (pH_{zpc}) results for the three treatments demonstrate dramatic changes occurring outside the useful pH range of the glass electrode (Table 4). It should be noted that these apparent zero point of charge values are not true zero points of charge because these experiments were performed at only one ionic strength and thus, the observed charges are apparent, not absolute charge (Plette et al., 1995).

There is an ~4-log-unit decrease in the value of the apparent pH_{zpc} from the MnO_{XW} (6.82) to MnO_{XD} (3.2), with the MnO_{XC} value (5.05) indicating again, reversibility in surface acid-base characteristics with re-wetting. The decrease in the pH_{zpc} with drying is consistent with Parks's (1965) finding which also observed that surface dehydration often results in a more acidic pH_{zpc}. This effect has been attributed to the aging of freshly precipitated manganese oxyhydroxides to a more stable, i.e., more crystalline form (Murray, 1974). It is difficult to rationalize the change in pH_{zpc} from the pK_a spectra. The model (Eqn. 2) assumes neutral sites deprotonating to form negatively charged sites but sites on minerals may be amphoteric (Dzombak and Morel, 1990) and thus a positively charged site deprotonating to form a neutral species is also possible. The pK_a values determined are independent of which reaction actually occurs. The shift in pH_{zpc} can be loosely interpreted by considering the S_o term in the equilibrium model (Eqn. 1). This term corresponds to the difference between the sites that are always positive and the sites that are always negatively charged over the entire titration range. The sites that are always negatively charged can be viewed as strong acid sites (easily deprotonated) and the sites that are always positively charged can be viewed as strongly basic sites (strongly held proton). The MnO_{XW} sample has the largest S_o value (2.1 ± 0.1 μmol/mg) and the MnO_{XD} sample has the smallest (0.07 ± 0.03 μmol/mg) with the cycle sampling coming in between (1.0 ± 0.2 μmol/mg). Thus, MnO_{XW} has the largest difference between sites that are always positive and those that are always negative and the dry sample has the smallest difference. It is difficult to say anything about the nature of these sites or their absolute concentrations because S_o corresponds to a difference, but it is possible to consider that either the MnO_{XW} has more strongly basic sites outside the titration range than the MnO_{XD}, and/or, the MnO_{XD} sample has more strongly acidic sites than the MnO_{XW}. The cycle treatment has an apparent pH_{zpc} intermediate to the wet and the dry treatments, indicating that the creation or loss of sites due to drying is, to a certain extent, a reversible process, upon rehydration. These results indicate, however, that a shift in the observed types of sites associated with hydrologic conditioning, must be balanced against the significant loss of sites observed with drying of the Mn oxyhydroxides (Table 4).

These results also have strong implications for sample storage and handling of amorphous mineral phases, especially since many analytical techniques require either a wet or dry sample. Our results show sample preparation will alter the characteristics of interest (e.g., surface reactivity, surface area, etc). While many researchers have noted the impact of aging on synthesized manganese oxyhydroxides (Murray et al., 1985; Catts and Langmuir, 1986; Mandernack et al., 1995) and some have indicated the effect of drying (Ross et al., 2001a), the influence of repeated dehydration and rehydration has received, until now, no quantitative investigation.

Hydroxyl functional groups associated with Fe oxyhydroxides are often observed in surface investigations to have pK_a values in the range of 4 to 11 (Cerník et al., 1996; Venema et al., 1998; Smith and Ferris, submitted). A spectrum of types of OH^- groups as indicated by varying pK_a values, implies differing properties from one OH^- group to the next as has been shown in many studies for metal oxyhydroxides (Smith and Ferris, submitted; Benjamin and Leckie, 1981; Catts and Langmuir, 1986; Venema et al., 1998). Generally, these results are interpreted to represent differing configuration of the surface hydroxyl groups, e.g., edge or dislocation sites on the mineral surface, which influences their resulting acidity. Our results provide new evidence that surface sites on amorphous surfaces are affected by hydrological variability. Our results showing both a decrease in total sites with drying despite increasing surface area (Tables 1 and 2), and a change in both the number and associated densities of differing types of sites (Table 3) clearly indicate that co-ordinational changes in the surface functional groups must occur with exposure to hydrologic change.

The nature and number of Mn and O bond associations at a particle surface will likely affect the acid base characteristics of those functional groups. Variations in bond lengths, co-ordinational associations and proximities of hydroxyl groups due to surface microstructure, will influence a number of processes, e.g., electron sharing, steric hindrance, interatomic interactions, all of which ultimately influence the associated acidity of those functional groups (Venema et al., 1998). This effect may be a result of the molecular configuration causing some OH^- groups to be bound more strongly (or weakly) than others. Catts and Langmuir (1986) noted that the structure of solid sorbent

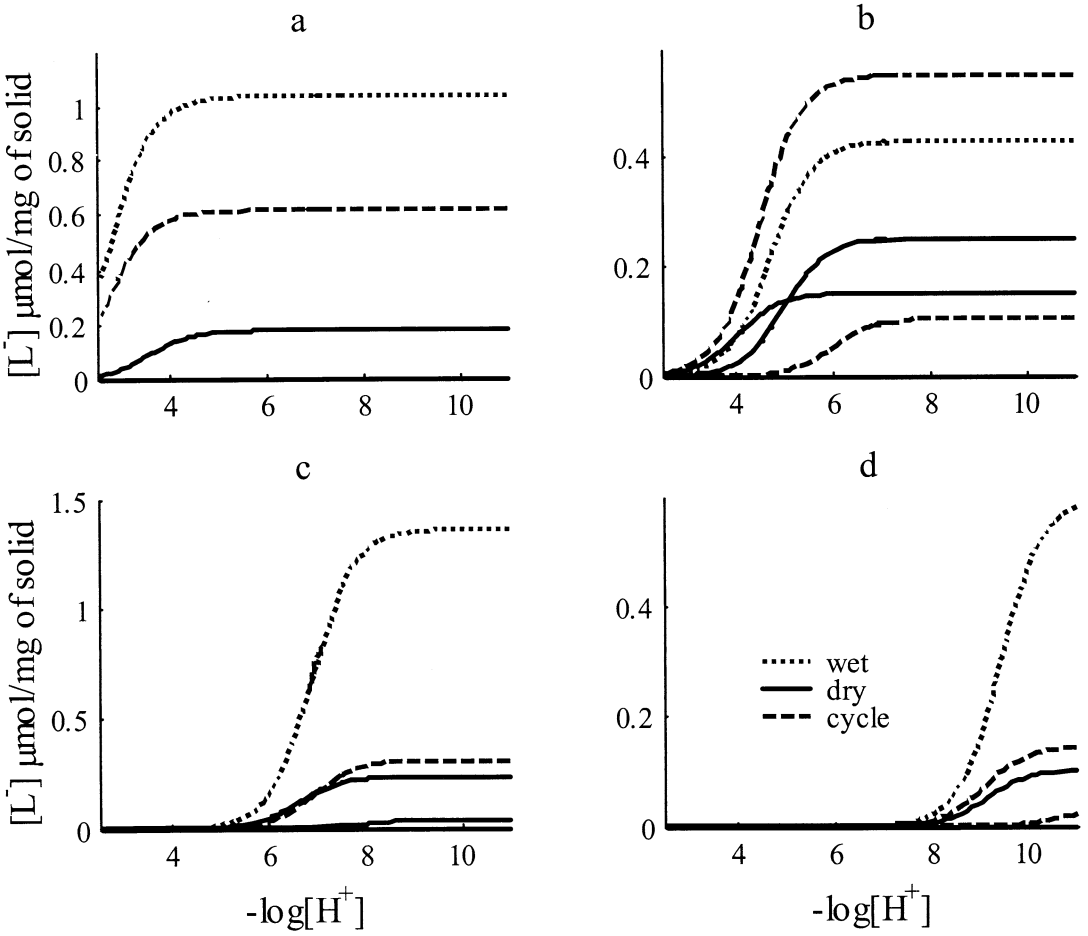

Fig. 3. Site speciation results for four classes of proton binding sites in the MnOx samples; the deprotonated species concentration is plotted as a function of pH. Subplots (a), (b), (c) and (d) correspond to type I, II, III and IV sites as indicated in the text. The sample identities of the different line styles are indicated on the figure. Note some sample types have more than one binding site of the indicated type.

surfaces have inhomogeneities that can result in several types of surface sites. X-ray absorption near edge structure (XANES) spectra have been used by other researchers to evaluate oxidation states which relate to the electron binding strength (Kay et al., 2001; Matocha et al., 2001; Ross et al., 2001a, 2001b). Manganese oxyhydroxides are redox sensitive, and can exist as either Mn(III), or Mn (IV) or mixtures of Mn(III,IV) (Murray, 1985; Tebo et al., 1997), which ultimately will alter the stability and bonding of adsorbed species (Davis and Kent; 1990; Hem, 1978). Other studies have considered the notion of high and low energy sites (Benjamin and Leckie, 1981; Post and Veblen, 1990; Matocha et al., 2001) and the growing evidence of pK_a spectrums for hydroxyl groups on Fe and Mn oxyhydroxide surfaces is at least, consistent with this idea. Benjamin and Leckie (1981) proposed that the high energy sites were occupied first, followed by lower energy sites, and thus, metal behaviour would be impacted by the relative number of high and low energy sites associated with any given mineral surface. Preliminary X-ray absorption spectroscopic analyses (XAS; GSECARS Beamline13; Advanced Photon Source, APS, Argonne; data not shown) of our Mn oxyhydroxide treatments indicates that all Mn oxyhydroxides are Mn (IV) oxidation state and thus, surface reactivity differences are not due to oxidation state differences. Whilst we cannot evaluate the relative changes in energies of various hydroxyl groups in our study, our results do clearly indicate that physical changes in surface acid base characteristics occur, which are dynamically reversible with variable hydrologic exposure. These results suggest that metal sorption by amorphous Mn oxyhydroxides is also likely to be impacted by hydrologically variable conditions.

The total proton binding capacity of these prepared Mn oxyhydroxides are similar to both hydrous ferric oxide and bacteria (Smith and Ferris, 2003). For comparison the sum of the proton binding sites for hydrous ferric oxide is 2.45 and for *Shewanella alga* strain CN32 the capacity is 2.18 μmol/mg of solid vs. 0.96 μmol/mg for our MnO_{XD} and 3.43 μmol/mg for our MnO_{XW}. These comparisons only compare the site density within the titratable range though and cannot compare differences in concentrations of very acidic or very basic sites. However, the apparent pH_{zpc} results of this study would suggest a stronger sorptive capacity of Mn oxyhydroxides at lower pH values compared to Fe oxyhydroxides as has been noted by other authors (Nelson et al., 1996; Tebo et al., 1997).

Table 4. Sites detected above and below the pH_{zpc} for each of the hydrological treatments.

	Sites detected below pH_{zpc} (μmol/mg)	pH_{zpc}	Sites detected above pH_{zpc} (μmol/mg)
MnO_{XW}	2.1 ± 0.1	6.82 ± 0.06	1.305 ± 0.008
MnO_{XD}	0.04 ± 0.02	3.2 ± 0.3	0.92 ± 0.05
MnO_{XC}	1.0 ± 0.2	5.05 ± 0.05	0.71 ± 0.03

3.3. Ni Sorption

Potential Mn oxide mineral dissolution associated with the low pH conditions of the Ni sorption experiments was negligible at both nominal pH values (<1% at pH 5, <2% at pH 2). However, it was treatment dependent (wet was most sensitive; dry was least sensitive), thus sorbent mass values have been corrected for dissolution loss. While potential Mn oxyhydroxide mass loss associated with dissolution was not directly measured in the titration experiments; these results indicating minimal dissolution over much longer time periods (24 vs. 2 h below pH 5 in the titration experiments) indicate that negligible dissolution is likely to have occurred. Other authors have reported dissolution of Mn oxyhydroxides. Loganathan and Burau (1973) examined dissolution of crystalline Mn oxyhydroxide material, which would likely exhibit different solubility than amorphous Mn oxyhydroxides. Further, they examined time dependent, rather than pH dependent, solubility. Whilst dissolution was minimal under the experimental timeframe of this study (<2% of total Mn mass at pH 5 and < 5% of total Mn mass at pH 2), the differential dissolution observed amongst the three Mn oxyhdyroxide treatments implies that hydrologic variability will impact not only the surface characteristics of amorphous minerals, but also their susceptibility to dissolution under low pH conditions in natural environments.

Differences in the amount of Ni sorbed amongst the three Mn oxyhydroxides were observed at both pH values examined (nominal pH 2 and 5; Fig. 4) if one standard error confidence intervals are assumed. While the results at pH 5 were consistent with the sorptive capacities implied by the determined surface characteristics above (i.e., wet > cycle > dry), the Ni sorption results at pH 2 were surprising. At pH 2, the MnO_{XW} which exhibited the highest total number of binding sites but a higher apparent pH_{zpc} of 6.82 ± 0.06 (Tables 2 and 4), sorbed significantly less Ni (0.42 ± 0.01 μmol/g) than either the MnO_{XC} treatment (0.48 ± 0.02 μmol/g), which had approximately half the total number of sites of the wet treatment, but a lower apparent pH_{zpc} of 5.05 ± 0.05, or the MnO_{XD} treatment (non-significant difference with wet treatment; 0.43 ± 0.01 μmol/g), which had the lowest number of sites (only 25% of the total number observed for the wet treatment (Table 2), but a much lower apparent pH_{zpc} of 3.2 ± 0.3, (Fig. 2). These results are consistent with the idea that hydroxyl surface groups exhibit differing site energies and affinities for metals and highlight the utility of using pK_a spectrum modeling to assess oxide mineral surface acid base characteristics. In addition, the lower Ni binding of the wet treated sample is consistent with the charging behaviour (Fig. 1) showing a net positive charge on the mineral surface.

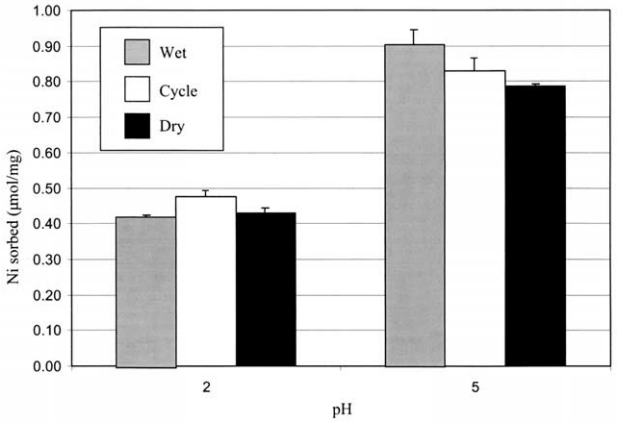

Fig. 4. Ni sorption data for all three experimental systems as a function of pH. Standard error bars calculated for treatment means, have been used to identify significant differences amongst treatments and pH values for a given treatment. Note that the variability in actual pH values among replicate samples was too small to be illustrated in this figure.

The quantity of Ni sorbed at pH 2, for all treatments, far exceeded the predicted capacity as determined by the surface characteristics and proton binding capacity. Under the same ionic strength, Murray (1974) determined adsorption of Ni to release of protons was a 1:1 ratio, which is consistent with McKenzie's (1979) determination of a single proton release during cation adsorption at pH 4 with a 0.26 mol/L electrolyte. However, our results for pH 2 show a greater ratio of Ni sorption to proton loss of 60:1 for MnO_{XW}, 92:1 for MnO_{XC} and an undefinable ratio for MnO_{XD} (zero proton binding sites were measured [Table 3] yet Ni sorption did occur [Table 5]). This result can be interpreted as a selective outcompeting of Ni for sites at low pH values, or that more sites exist below the titratable range (pH 2–10) as suggested by the apparent pH_{zpc} results (Table 4), which we cannot quantify. In addition, Ni may be associating with the surface as a precipitate rather than as a chemically bound species. If that is the case then the Ni binding capacity could exceed the proton binding capacity. These questions will be addressed in a future communication on XAS investigation of these solids.

In the pH 5 experiment, all three Mn oxyhydroxides treatments showed higher sorption of Ni, approximately doubling the sorptive capacities compared to pH 2, as would be expected, due to a higher number of negative sites (Table 5, Fig. 2). However, the highest sorption was observed for the wet treatment, followed by the cycle and the dry (MnO_{XW} [0.90 ± 0.04 μmol/g]; MnO_{XC} [0.83 ± 0.04 μmol/g]; and MnO_{XD} [0.79 ± 0.01 μmol/g]; Table 5). MnO_{XW} sorbed significantly more than the MnO_{XD} at the one standard error confidence interval, but no significant differences were observed between MnO_{XC} and either MnO_{XD} or MnO_{XW} (Table 5). Thus drying of the Mn oxyhydroxides significantly decreased the sorptive capacity at pH 5, whilst re-wetting increased the sorptive capacity back to similar values for the wet, non-dried Mn oxyhydroxides.

While the actual Ni sorption at pH 5, was significantly different than that predicted by the proton binding capacity for each of the treatments, the Ni sorption was in the same mag-

Table 5. Ni sorption vs. capacity at pH 2 and 5 for the three hydrological treatments (all units are μmol/mg).

	pH 2		pH 5	
	Ni sorption	Proton binding capacity	Ni sorption	Proton binding capacity
MnO_{XW}	0.42 ± 0.01	0.0068 ± 0.0007	0.90 ± 0.04	1.39 ± 0.05
MnO_{XD}	0.43 ± 0.01	0	0.79 ± 0.01	0.46 ± 0.03
MnO_{XC}	0.48 ± 0.02	0.005 ± 0.003	0.83 ± 0.04	1.0 ± 0.2

nitude as that predicted and followed the same trend in terms of Wet > Cycle > Dry. This result is consistent with the study by Kay et al. (2001) where Ni uptake by Mn oxyhydroxides in a Pinal Creek, Globe Mining District, was observed to be almost completely reversible, indicating that Ni reacted primarily with reversible sorption sites. Therefore, as the Mn oxyhydroxides are dried, proton binding sites are lost, which impacts their Ni sorption capacity; however upon rehydration some of the sites are restored and Ni scavenging abilities increase, illustrating a reversible process.

These results indicate that whilst pH will impact Ni sorption to oxyhydroxides, the impact will differ depending on the pH examined, reflecting differences in the nature of the surface characteristics of the oxide surface. Our results show that hydrologic conditioning shifts the types and numbers of surface sites and thus, the pH effect on sorption is different for each treatment. At the more basic pH of 5, the wet treatment, which has a higher proportion of basic sites (Table 3), sorbs more Ni compared to the other two Mn oxyhydroxides treatments (Table 5). However, at pH 2, the MnO_{XC} and MnO_{XD} sorb more Ni compared to the MnO_{XW}. Thus, the total number of proton sites estimated from the titratable range, by itself, is not a sensitive indicator of metal sorption characteristics.

The high Ni:Mn ratio was purposely chosen to reflect the extremely high concentrations of Ni and the relatively small amount of solid mass of Mn oxyhydroxides commonly observed in the on-going field investigation. Nickel sorption to amorphous Mn oxyhydroxides in the field site plateaus at a 10:1 mol/L ratio of Ni:Mn (Haack and Warren, 2003). Thus, in this laboratory study we used a similar Ni:Mn molar ratio to mimic the field conditions. Furthermore, the high Ni concentration was expected to saturate the low pK_a sites, thus proton binding capacity would be expected to predict Ni sorption results. Likewise, the pH range examined (2–5), reflects ambient conditions observed in the field site (Haack and Warren, 2003). Unfortunately, due to the extreme paucity of published laboratory studies evaluating metal sorption to Mn oxyhydroxides under low pH and variable hydrologic regimes, relevant comparison of these results to published values for Ni sorption is extremely limited. While Trivedi and Axe (2001) found adsorption capacity of hydrous metal oxides of manganese, iron and aluminium to follow the order manganese oxyhydroxide > iron oxyhydroxide > aluminium oxyhydroxide, the circumneutral pH and the low initial metal concentrations prohibit any meaningful comparison between studies. Trivedi et al. (2001) also examined Ni sorption to manganese oxyhydroxides and found values one to two orders of magnitude larger than those reported in this study; however, given their long storage time and metal exposure times (up to 110 d) as well as the circumneutral pH conditions, sorption values would be expected to differ significantly especially since we have demonstrated sample history strongly affects mineral sorption characteristics. However, field investigation under low pH conditions (Haack and Warren, 2003) show biofilm associated, biogenic amorphous Mn oxyhydroxide Ni sorptive capacities to be of the same order of magnitude (~0.2 μmol/mg) to those determined for our laboratory synthetic Mn oxyhydroxides (0.41–1.39 μmol/mg).

4. CONCLUSIONS

Variable wetting and drying regimes do not affect bulk crystallinity of synthetic Mn oxyhydroxides; but induce reversible changes in surface acid base characteristics. The high reproducibility of the acid-base titrations and the strong fit between the experimental data and the modelled data for the three Mn oxyhydroxides that had undergone conditioning to represent three different hydrologic regimes (MnO_{XW}, MnO_{XC} and MnO_{XD}), indicate that their surface characteristics are robust despite their amorphous nature. Drying of the Mn oxyhydroxides decreased the total number of proton binding sites. Cyclically rewetting and drying did not change surface area from that of dried Mn oxyhydroxides, but did produce an intermediate total proton binding site density to that of fresh wet Mn oxyhydroxides and dried Mn oxyhydroxides. Thus, whilst drying increases the relative surface area, it decreases the density of sites per unit surface area suggesting co-ordinational differences in the hydroxyl surface functional groups occur. The physical surface characteristics indicate that while surface area consistently increases with repeated drying and wetting, the loss of proton binding sites with drying is reversible upon rehydration ($MnO_{XW} > MnO_{XC} > MnO_{XD}$). These results show that surface particle size is controlled by drying and is not sensitive to rewetting; whilst surface acid base characteristics are sensitive to rewetting. Further, a shift in the types and associated densities with hydrologic conditioning was observed. Apparent pH_{zpc} values decreased from 6.82 ± 0.06 for the wet to 3.2 ± 0.3 for the dry and then increased again to 5.05 ± 0.05 for the cycle treatment, which can possibly be accounted for by the creation of strong acid sites < pH 2 with drying of the Mn oxyhydroxide.

The Ni sorption results showed higher Ni sorption in all three Mn oxyhydroxides treatments at pH 5 compared to pH 2 as would be expected. However, the trend of which Mn oxyhydroxide treatment sorbed the most differed between the two pH values. This result reflects the changes in types and densities of surface functional gropus induced by hydrologic conditioning. Ni sorptive capacities were determined to be highest for

MnO_{XW} followed by MnO_{XC} and the MnO_{XD}, at pH 5, whilst at pH 2, Ni sorption was highest for $MnO_{XC} + MnO_{XD}$, which were greater than that observed for MnO_{XW}. This study is the first to our knowledge, to quantitatively examine the impact of hydrologic variability on both particle characteristics of size, surface area and acid-base characteristics, and associated metal sorptive capacities. Our results indicate that hydrologic variability in natural environments will impact metal behaviour and that this behaviour is consistent with observed changes in acid base characteristics of the surface. This finding can be expected to extend to other amorphous metal oxyhydroxides such as those of Fe. While there is a large body of knowledge on both the structure and reactivity of Fe oxyhydroxides, the impact of hydrologic variability has yet to be considered. The surface coordinational environments of these Mn oxyhydroxides will be the subject of a future communication employing XAS to determine the coordinational environments of surface functional groups for these three hydrologically conditioned Mn oxyhydroxides.

Acknowledgments—Funding support for this work was provided by NSERC, CFI, and OIT to LAW. CK was supported by an NSERC undergraduate summer fellowship for a portion of this work. Comments provided by Dr. Pat Brady, Dr. Roy Wogelius and an anonymous reviewer greatly improved the final manuscript. We gratefully acknowledge the analytical support provided by Falconbridge Ltd in this research. XRD and SEM analyses were carried out by Shirley Lalonde, of the Falconbridge Technology Centre, Sudbury, ON, Canada.

Associate editor: R. A. Wogelius

REFERENCES

Appelo C. A. J. and Postma D. (1999) A consistent model for surface complexation on birnessite (-MnO_2) and its application to a column experiment. *Geochim. Cosmochim. Acta* **63,** 3039–3048.

Benjamin M. M. and Leckie J. O. (1981) Multiple-site adsorption for Cd, Cu, Zn, and Pb on amorphous iron oxyhydroxide. *J. Colloid Interface Sci.* **79,** 209–221.

Bond P. L., Smriga S. P., and Banfield J. F. (2000) Phylogeny of microoganisms populating a thick, subaerial, predominantly lithotrophic biofilm at an extreme acid mine drainage site. *Appl. Ennviron. Microbiol.* **66,** 3842–3849.

Brassard P., Kramer J. R., and Collins P. V. (1990) Binding site analysis using linear programming. *Environ. Sci. Technol.* **24,** 195–201.

Catts J. G. and Langmuir D. (1986) Adsorption of Cu, Pb and Zn by MnO2: applicability of the site binding-surface complexation model. *Appl. Geochem.* **1,** 255–264.

Cerník M., Borkovec M., and Westall J. C. (1995) Regularized least-squares method for the calculation of discrete and continuous affinity distributions for heterogeneous sorbents. *Environ. Sci. Technol.* **29,** 413–425.

Cerník M., Borkovec M., and Westall J. C. (1996) Affinity distribution description of competitive ion binding to heterogeneous materials. *Langmuir* **12,** 6127–6137.

Cox J. S., Smith D. S., Warren L. A., and Ferris F. G. (1999) Characterizing heterogeneous bacterial surface functional groups using discrete affinity spectra for proton binding. *Environ. Sci. Technol.* **33,** 4514–4521.

Davis J. A. and Kent D. B. (1990) Surface complexation modelling in aqueous geochemistry. *Rev. Mineral.* **23,** 177–260.

Dzombak D. A. and Morel F. M. M. (1990) *Surface Complexation Modeling: Hydrous Ferric Oxide*. Wiley-Interscience, New York.

Emerson D. (2000) Microbial oxidation of Fe(II) and Mn(II) at circumneutral pH. In *Environmental Microbe-Metal Interactions* (ed. D. R. Loveley), pp. 31–52. ASM Press, Washington, DC.

Emerson S., Kalhorn S., and Jacobs L. (1982) Environmental oxidation rate of manganese (II): Bacterial catalysis. *Geochim. Cosmochim. Acta* **46,** 1073–1079.

Fein J. B., Daughney C. J., Yee N., and Davis T. A. (1997) A chemical equilibrium model for metal adsorption onto bacterial surfaces. *Geochim. Cosmochim. Acta* **61,** 3319–3328.

Fritsch S., Post J. E., and Navrotsky A. Energetics of low temperature polymorphs of manganese dioxide and oxyhydroxide. *Geochim. Cosmochim. Acta* **61,** 2613–2616.

Haack E. A. and Warren L. A. (2003) Biofilm hydrous manganese oxyhydroxides and metal dynamics in acid rock drainage. *Env. Sci. Technol.* **37,** 4138–4147.

Hem J. D. (1978) Redox processes at surfaces of manganese oxide and their effects on aqueous metal ions. *Chem. Geol.* **21,** 199–218.

Kay J. T., Conklin M. H., Fuller C. C. and O'Day P. A. (2001) Processes of nickel and cobalt uptake by a manganese oxide forming sediment in Pinal Creek, Globe Mining District, Arizona. *Environ. Sci. Technol.* **35,** *24,* 4719–4725.

Kukier U. and Chaney R. L. (2000) Remediating Ni-phytotoxicity of contaminated quarry muck soil using limestone and hydrous iron oxide. *Can. J. Soil Sci.* **80,** *4,* 581–593.

Kusel K. and Dorsch T. (2000) Effect of supplemental electron donors on the microbial reduction of Fe(III), sulfate and CO_2 in coal mining-impacted freshwater lake sediments. *Microbial Ecol.* **40,** *3,* 238–249.

Lee G., Bigham J. M., and Faure G. (2002) Removal of trace metals by coprecipitation with Fe, Al and Mn from natural waters contaminated with acid mine drainage in the Ducktown Mining District, Tennessee. *Appl. Geochem.* **17,** 569–581.

Leveille S. A., Leduc L. G., Ferroni G. D., Telang A. J., and Voordouw G. (2001) Monitoring of bacteria in acid mine environments by reverse sample genome probing. *Can. J. Microbiol.* **47,** 431–442.

Loganathan P. and Burau R. G. (1973) Sorption of heavy metal ions by a hydrous manganese oxide. *Geochim. Cosmochim. Acta* **37,** 1277–1293.

Luo J. Q., Zhang C., and Suib S. L. (2000) Mechanistic and kinetic studies of crystallization of birnessite. *Inorg. Chem.* **39,** 741–747.

Mandernack K. W., Post J., and Tebo B. M. (1995) Manganese mineral formation by bacterial spores of the marine *Bacillus*, strain SG-1: Evidence for the direct oxidation of Mn(II) to Mn(IV). *Geochim. Cosmochim. Acta* **59,** 4393–4408.

Matocha G. J., Elzinga E. J., and Sparks D. L. (2001) Reactivity of Pb(II) at the Mn(III,IV) (oxyhydr)oxide-water interface. *Environ. Sci. Technol.* **35,** 2967–2972.

McKenzie R. M. (1979) Proton release during adsorption of heavy metal ions by a hydrous manganese dioxide. *Geochim. Cosmochim. Acta* **43,** 1855–1857.

Murray J. W. (1974) The surface chemistry of hydrous manganese dioxide. *J. Colloid Interface Sci.* **46,** 357–371.

Murray J. W., Dillard J. G., and Giovanoli R. (1985) Oxidation of Mn(II): Initial mineralogy, oxidation state and ageing. *Geochim. Cosmochim. Acta* **49,** 463–470.

Nederlof M. M., van Riemsdijk W. H., and Koopal L. K. (1994) Heterogeneity analysis for binding data using an adapted smoothing spline technique. *Environ. Sci. Technol.* **28,** 1037–1047.

Nelson Y. M., Lion L. W., Ghiorse W. C., and Shuler M. L. (1996) Modeling oligotrophic biofilm formation and lead adsorption to biofilm components. *Environ. Sci. Technol.* **30,** 2027–2035.

Nelson Y. M., Lion L. W., Ghiorse W. C., and Shuler M. L. (1999a) Production of biogenic Mn oxides by *Leptothrix discophora* S-1 in a chemically defined growth medium and evaluation of their Pb adsorption characteristics. *Appl. Environ. Microbiol.* **65,** 175–180.

Nelson Y. M., Lion L. W., Schuler M. L., and Ghiorse W. C. (1999b) Lead binding to metal oxide and organic phases of natural aquatic biofilms. *Limnol. Oceanogr.* **44,** 1715–1729.

Nelson Y. M., Lion L. W., Shuler M. L., and Ghiorse W. C. (2002) Effect of oxide formation mechanisms on lead adsorption by biogenic manganese (hydr)oxides, iron (hydr)oxides, and their mixtures. *Environ. Sci. Technol.* **36,** 421–425.

Parks G. A. (1965) The isoelectric points of solid oxides, solid hydroxides and aqueous hydroxo complex systems. *Chem. Rev.* **65,** 177–198.

Parmar N., Borby Y. A., Beveridge T. J., and Ferris F. G. (2001) Formation of green rust and immobilization of nickel in response to bacterial reduction of hydrous ferric oxide. *Geomicrobiol. J.* **18,** *4,* 375–385.

Plette A. C. C., van Riemsdijk W. H., Benedetti M. F., and van der Wal A. J. (1995) pH dependent charging behaviour of isolated cell walls of a gram-positive soil bacterium. *J. Colloid Interface Sci.* **173,** 354–363.

Post J. E. and Velben D. R. (1990) Crystal structure determinations of synthetic sodium magnesium and potassium birnessite using TEM and the Rietveld method. *Am. Mineral.* **75,** *5–6,* 477–489.

Press W. H., Teukolsky S. A., Vetterling W. T., and Flannery B. P. (1992) *Numerical Recipes in FORTRAN: The Art of Scientific Computing*. 2nd ed. Cambridge University Press, Cambridge, UK.

Robertson A. P. and Leckie J. O. (1998) Acid/base, copper binding, and Cu^{2+}/H^{+} exchange properties of goethite, an experimental and modeling study. *Environ. Sci. Technol.* **32,** 2519–2530.

Ross D. S., Hales H. C., Shea-McCarthy G. C. and Lanzirotti A. (2001a) Sensitivity of soil manganese oxides: Drying and storage cause reduction. *Soil Sci. Soc. Am. J.* **65,** *3,* 736–743.

Ross D. S., Hales H. C., Shea-McCarthy G. C., and Lanzirotti A. (2001b) Sensitivity of soil manganese oxides: XANES spectroscopy may cause reduction. *Soil Sci. Soc. Am. J.* **65,** *3,* 744–752.

Schwertmann U. and Cornell R. M. (1991) *Iron Oxides in the Laboratory*. VCH, New York.

Smith D. S. and Ferris F. G. (2003) Specific surface chemical interactions between hydrous ferric oxide and iron-reducing bacteria determined using pKa spectra. *J. Colloid Interface Sci.* **266,** 60–67.

Tebo B. M., Ghiorse W. C., van Waasbergen L. G., Siering P. L., and Caspi R. (1997) Bacterially mediated mineral formation: In-sights into manganese (II) oxidation from molecular genetic and biochemical studies. *Rev. Mineral.* **35,** 225–266.

Tessier A., Fortin D., Belzile N., DeVitre R. R., and Leppard G. G. (1996) Metal sorption to diagenetic iron and manganese oxyhydroxides and associated organic matter: Narrowing the gap between field and laboratory measurements. *Geochim. Cosmochim. Acta* **60,** 387–404.

Trivedi P. and Axe L. (2001) Predicting divalent metal sorption to hydrous Al, Fe, and Mn oxides. *Environ. Sci. Technol.* **35,** 1779–1784.

Trivedi P., Axe L., and Tyson T. A. (2001) XAS studies of Ni and Zn sorbed to hydrous manganese oxide. *Environ. Sci. Technol.* **35,** 4515–4521.

Venema P., Hiemstra T., Weidler P. G., and van Riemsdijk W. H. (1998) Intrinsic proton affinity of reactive surface groups of metal (hydr)oxides: Application to iron (hydr)oxides. *J. Colloid Interface Sci.* **198,** 282–295.

Warren L. A. and Ferris F. G. (1998) Continuum between sorption and precipitation of Fe(III) on microbial surfaces. *Environ. Sci. Technol.* **32,** 2331–2337.

Zar J. H. (1984) *Biostatistical Analysis*. 2nd ed. Prentice-Hall, Englewood Cliffs, NJ.